Luminescence spectra of quantum dots in microcavities. III. Multiple quantum dots

F. P. Laussy,[1,*] A. Laucht,[1] E. del Valle,[2] J. J. Finley,[1] and J. M. Villas-Bôas[1,3]

[1]*Walter Schottky Institut, Technische Universität München, Am Coulombwall 3, D-85748 Garching, Germany*

[2]*Physikdepartment, Technische Universität München, James-Franck-Straße 1, D-85748 Garching, Germany*

[3]*Instituto de Física, Universidade Federal de Uberlândia, CEP 38400-902 Uberlândia, Minas Gerais, Brazil*

(Received 27 March 2011; revised manuscript received 28 September 2011; published 9 November 2011)

We discuss the spectral line shapes of N quantum dots in strong coupling with the single mode of a microcavity in the presence of a continuous, incoherent pumping. Nontrivial features in the response of the system are induced by detuning the emitters or probing the direct exciton emission spectrum. We describe dark states, quantum nonlinearities, emission dips, and interferences and show how these various effects may coexist, giving rise to highly peculiar line shapes.

DOI: 10.1103/PhysRevB.84.195313 PACS number(s): 42.50.Ct, 42.70.Qs, 71.36.+c, 78.67.Hc

I. INTRODUCTION

The coherent coupling of *one* semiconductor quantum dot (QD) exciton to the optical mode of a microcavity has been intensely investigated over the last years in cavity quantum electrodynamics (cQED) experiments[1–20] and theory.[21–40] The possibility of coupling strongly more than one quantum dot to the (still single) microcavity mode[40–48] is starting to emerge experimentally,[4,19,49,50] as technology makes always more accessible the design and control of complex configurations with multiple quantum dots.[51,52] The rich physics of the single-quantum-dot case is thus finding an even richer and wider arena where $N > 1$ dots are simultaneously involved. This echoes the theoretical route taken by the fathers of this field with the Tavis-Cummings model[53] in 1968 extending to N atoms the Jaynes-Cummings model[54] of 1963, which considers the case of a single emitter.

A typical characterization of quantum dots in a microcavity is through photoluminescence: the system is excited incoherently and its luminescence is detected as a function of the energy of the emitted photons. The single-quantum-dot case displays much of the behaviors that are generalized with N emitters, so it is helpful to review them here. The experimentally obtained spectral shapes of strongly coupled QD-cavity systems have been directly compared to a theoretical model,[11,12,19,23] and the agreement is excellent. It was assumed in these cases that most of the light escapes the system via the radiation pattern of the cavity mode, and the experimental spectra were compared to the spectral function calculated from the cavity occupation. This detection geometry is known in atomic cQED as "end emission" or "forward emission."[55] In atomic systems, a negligible fraction of the light escapes the cavity through the cavity mode; that is to say, the cavity photon lifetime is so long that it can be considered infinite. Light is then detected in the so-called side-emission geometry, where the radiation pattern of the emitter is directly probed. With microcavities, the situation is reversed: the cavity mode is measured and the emitter has typically a much longer lifetime. In the spontaneous emission regime, this makes measurements of the Rabi doublet in the photoluminescence more difficult, unless some cavity feeding makes the quantum state of the system photonlike.[23] This is because changing the nature of the excitation is, in the linear regime, equivalent to changing the channel of detection.[27] In the nonlinear regime, this also hinders the observation of the quantized structure of the energy levels, the celebrated Jaynes-Cummings ladder. There are four possible transitions between consecutive rungs of the ladder and these have the same intensity in the exciton emission but different intensities in the cavity emission. This is because in the cavity emission the photon has two paths to be emitted: one with the dot in its ground state, the other with the dot in its excited states.[28] These two paths interfere destructively when the initial and final states are out of phase, which is the case for two out of the four possible transitions, and constructively when the initial and final states are in phase, or, up to a photon, indistinguishable. In the dressed-state picture, the cavity photon to be emitted decouples from the polaritons and carries away little information from the coupled system, being more cavity-photonlike as the number of excitations becomes higher. On the other hand, the photon emitted directly by the dot does not decouple from the system, regardless of the number of excitations: the dot cannot lose its excitation without fundamentally altering the state of the entire system. As a result, the dot photon carries more information about the coupled system. Summarizing, the dot is essentially a quantum emitter whereas the cavity is essentially a classical emitter.

It is, therefore, extremely interesting to develop techniques to directly probe the dot(s) emission using an experimental geometry that excludes light arising from the cavity. The ratio $\mathcal{R}$ of photons emitted by one quantum dot compared with the cavity depends on the populations of the dot (n_1) and cavity (n_a), and their rate of emission, γ_1 and γ_a, respectively.

$$\mathcal{R} = \frac{n_1\gamma_1}{n_a\gamma_a}. \tag{1}$$

This ratio is typically small since—apart from the fact that $0 \leqslant n_1 \leqslant 1$, whereas n_a is unbounded—in typical experiments, $\gamma_1 \ll \gamma_a$. Therefore, one should take advantage of the detection geometry to detect light in a solid angle where the cavity does not emit. In a photonic crystal, one could try to filter out the areas of most intense cavity emission by selective collection of the far-field emission. This is, however, not efficient enough to compensate the several-order-of-magnitude difference in $\mathcal{R}$ (we estimate the ratio of cavity to dot emission by comparing the far-field emission pattern of an $L3$ cavity mode obtained from finite-difference time-domain simulations with the emission of an isotropic emitter. From assuming collection for different numerical apertures or blocking of these numerical

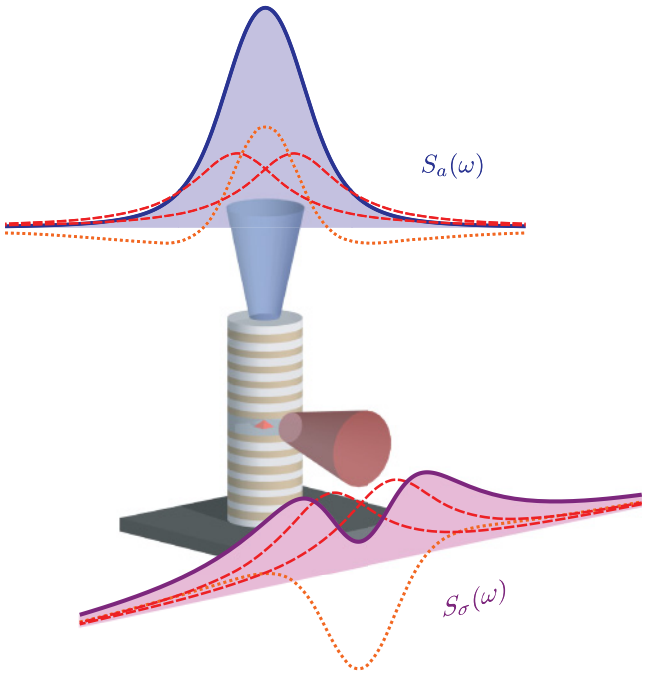

FIG. 1. (Color online) Sketch of the two main channels of emission from a quantum dot in a microcavity, here illustrated with a micropillar. The cavity emission, or end emission (S_a, in blue), emits along the axis of the structure. The QD emission, or side emission (S_σ, in purple), emits through the leaky modes (pictured as a beam). The emission spectra can be decomposed into their polariton emission [dashed (red) curves], which is intrinsic to the coupling inside the structure and is therefore identical in both cases. The channel of detection superimposes to the polariton emission an interference part [dotted (orange) curve], which summed with the polariton contribution provides the observed spectrum, the filled line shapes. For the parameters chosen, the Rabi splitting between polaritons is observed in the QD emission but not in the cavity emission.

apertures we could estimate a maximum inhibition of the cavity emission compared to the dot emission of a factor of ∼2.5.) The direct dot emission is therefore more easily accessible in a micropillar geometry,[56] where one can detect from the side of the structure, as depicted in Fig. 1. The feasibility of such experiments has already been demonstrated.[57] Figure 1 shows that the intrinsic polariton splitting [dashed (red) curves] is either magnified or washed away in the luminescence observed in the quantum dot [solid (purple) curve] or cavity [solid (blue) curve], respectively, as a result of the superimposed interference term [dotted (orange) curve]. In the case of the quantum dot emission, although the result is qualitatively similar in this case, it should not be trusted to provide accurate quantitative estimates.[58] In this text, we do not take further interest in the practical question of how to separately detect the dot(s) and cavity emission but show the differences that are observed when probing the strong-coupling physics in these two channels of emission. We revisit the case $N = 1$ to provide a background for the general case. With more than one quantum dot, we show that some of the physics observed in the direct quantum dot emission of the single emitter can be transferred to the cavity emission and therefore be easily detected experimentally. As in the previous parts of this work,[27,28] we address both the linear and nonlinear regimes (under incoherent and continuous pumping as the scheme of excitation) and focus on the line shape of the luminescence spectra. The effects we discuss are not limited to the case of quantum dots in a microcavity. Systems with many identical quantum emitters are equally well described by our formalism. Examples include atomic ensembles coupled to a high-finesse Fabry-Pérot cavity,[59,60] superconducting qubits coupled to a microwave resonator,[61–63] or an ensemble of color centers in diamond.[64–66]

II. MODEL

The Hamiltonian for N independent excitons (in different two-level systems QDs) coupled to a common cavity mode is merely a sum over the various emitters of the single QD Hamiltonian of Part II of this work:[28]

$$H = \sum_{j=1}^{N} [\omega_j \sigma_j^\dagger \sigma_j + g_j (a^\dagger \sigma_j + \sigma_j^\dagger a)] + \omega_a a^\dagger a, \qquad (2)$$

where $\sigma_j^\dagger$, σ_j are the pseudospin operators for the excitonic two-level systems consisting of the ground state $|0\rangle$ and a single exciton $|X_j\rangle$ state of the jth QD; ω_j is the exciton frequency, $a^\dagger$ and a are the creation and destruction operators of photons in the cavity mode with frequency ω_a, and g_j describes the strength of the dipole coupling between the cavity mode and the exciton of the jth QD. The incoherent loss and gain (pumping) of the dot-cavity system is included in a master equation of the Lindblad form $\frac{d\rho}{dt} = -i[H,\rho] + \mathcal{L}(\rho)$, where

$$\begin{aligned}\mathcal{L}(\rho) = \sum_{j=1}^{N} \Bigg[& \frac{\gamma_j}{2}(2\sigma_j \rho \sigma_j^\dagger - \sigma_j^\dagger \sigma_j \rho - \rho \sigma_j^\dagger \sigma_j) \\ & + \frac{P_j}{2}(2\sigma_j^\dagger \rho \sigma_j - \sigma_j \sigma_j^\dagger \rho - \rho \sigma_j \sigma_j^\dagger) \Bigg] \\ & + \frac{\gamma_a}{2}(2a\rho a^\dagger - a^\dagger a \rho - \rho a^\dagger a) \\ & + \frac{P_a}{2}(2a^\dagger \rho a - a a^\dagger \rho - \rho a a^\dagger). \end{aligned} \qquad (3)$$

Here, γ_j is the jth exciton decay rate, P_j is the rate at which excitons are created by a continuous-wave pump laser in the jth QD, γ_a is the cavity loss, and P_a is the incoherent pumping of the cavity. Pumping of the cavity from nonresonant QDs was observed and investigated by different groups.[5,14,15,67–72] It has been shown how the effective quantum state realized in the system under the interplay of the two types of pumping (cavity and exciton) imparts a strong influence on the line shape,[23] as detailed extensively previously.[27,28] In the linear regime, this is a counterpart of the different channels of emission. A pure dephasing rate of the exciton in the jth QD could be included to account for effects originating from high excitation powers or high temperatures.[11] However, such effects have a tendency to merge together the closely spaced peaks arising from higher rungs of the Jaynes-Cummings ladder,[73] and we neglect it here for the sake of simplicity.

Assuming that the system achieves a steady state for long times and employing the Wiener-Khintchine theorem, we

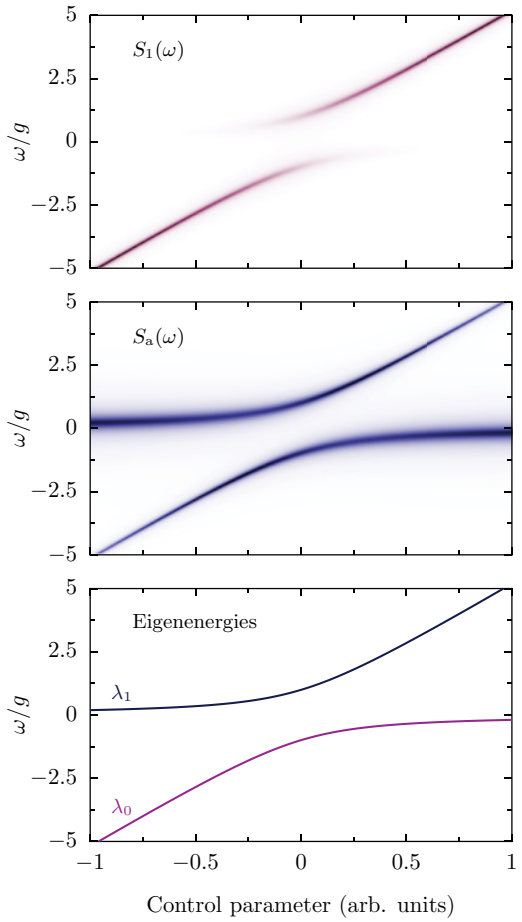

FIG. 2. (Color online) One dot in a cavity. Emission spectrum from the radiation channel of the exciton $S_1(\omega)$, from the radiation channel of the cavity mode $S_a(\omega)$, and eigenstates of the system. Parameters: $\gamma_a/g = 0.5$, $\gamma_1/g = 0.1$, $P_1/g = 10^{-3}$, and $P_a = P_1$.

calculate the spectral function[74] when photon emission occurs via the normalized radiation pattern of the cavity,

$$S_a(\omega) = \frac{1}{n_a \pi} \lim_{t\to\infty} \mathrm{Re} \int_0^\infty d\tau e^{-(\Gamma_R - i\omega)\tau} \langle a^\dagger(t) a(t+\tau)\rangle, \quad (4)$$

and via the normalized radiation pattern of the jth QD:

$$S_j(\omega) = \frac{1}{n_j \pi} \lim_{t\to\infty} \mathrm{Re} \int_0^\infty d\tau e^{-(\Gamma_R - i\omega)\tau} \langle \sigma_j^\dagger(t) \sigma_j(t+\tau)\rangle. \quad (5)$$

We included in the expression the term Γ_R that takes into account the finite spectral resolution of a monochromator,[75] which is 10 μeV (half-width) for a good monochromator by today's standards. The qualitative effect of this term is to broaden the peaks and blur the features. Therefore, in the following we assume it is zero (i.e., the case of a perfect detector).

Using the quantum regression theorem,[76] the emission eigenfrequency is obtained by solving the Liouvillian equations for the single time expectation value and has been amply detailed elsewhere.[77] Assuming that the emission energy of different QDs changes differently with respect to a control parameter, which is the case for electrically tuned QDs, we can bring two or more QDs into resonance at the same time. This can be simply modeled by an effective control parameter such as $\omega_j = \alpha_j V_{\mathrm{control}}$, where α_j gives the different slopes of emission frequency with the control parameter V_{control}. The emission frequency of the cavity mode is assumed not to be affected by this control parameter.

III. ONE EMITTER

We revisit the simplest and most popular case of one QD strongly coupled to the cavity mode. This was the system studied in the previous parts of this work.[27,28] As before, we compare the emission spectra of the cavity and dot emission, emphasizing results of interest that we find to be magnified in the case of multiple QDs. We plot in Fig. 2 the emission spectra from the radiation channel of the exciton $S_1(\omega)$, from the radiation channel of the cavity mode $S_a(\omega)$, and the eigenstates. Close to resonance, both the exciton and the cavity mode emit into both radiation channels and the radiation patterns are very similar [see also Fig. 3(a)]. Far away from resonance, the spectra look different, the excitonic channel $S_1(\omega)$ being dominated by the emission of the exciton and the cavity channel $S_a(\omega)$ being dominated by the cavity emission. However, a difference in the relative emission strengths cannot be directly attributed to a preference in the radiation channel. It is also dependent on the experimental parameters, on the

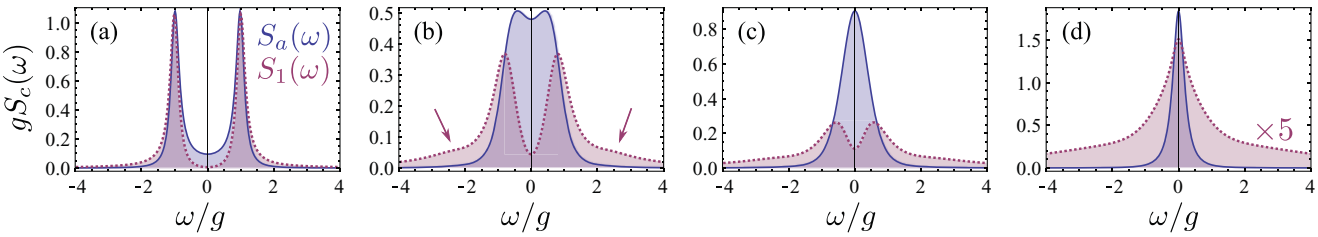

FIG. 3. (Color online) Cavity [solid (blue) curve] and dot [dotted (purple) curve] emission spectra for one dot in a cavity as a function of pumping power. In the spontaneous emission regime (a), there are no qualitative differences between the two types of spectrum. Increasing pumping (b)–(d) shows markedly different behaviors in the two channels of emission. Whereas the cavity spectrum does not present a particularly rich phenomenology (collapse of the Rabi doublet), the dot emission displays more characteristic line shapes. Side elbows are formed [outlined with arrows in (b)] and strong deviations from Lorentzian lines are obtained even when the spectrum has only one peak. Parameters: $\gamma_a/g = 0.5$, $\gamma_1/g = 0.1$, $P_a = 0$, and (a) $P_1/g = 10^{-3}$, (b) $P_1/g = 0.5$, (c) $P_1/g = 1$, and (d) $P_1/g = 2$.

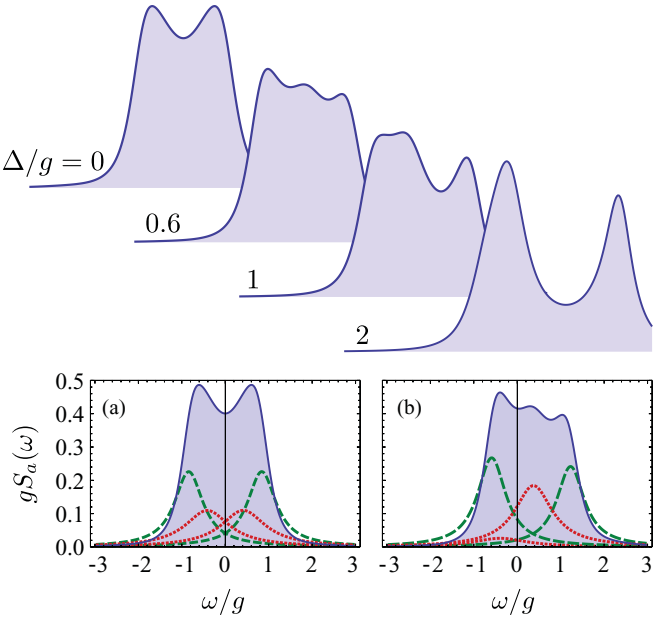

FIG. 4. (Color online) Cavity spectrum of one dot in a cavity as a function of detuning. Lower panels, decomposition of the spectrum in its dressed states emission lines [$|1,\pm\rangle \rightarrow |\text{vacuum}\rangle$, dashed (green) curve; and $|2,\pm\rangle \rightarrow |1,\pm\rangle$, dotted (red) curve], showing how (a) Jaynes-Cummings transitions are hindered at resonances but (b) are revealed out of resonance. Parameters are the same as in Fig. 3 but with the detunings $\Delta/g = 0$, 0.6, 1, and 2 and $P_1/g = 0.4$.

specific pumping rate of the exciton, on the number of other transitions or QDs feeding the cavity mode, and of course on the different coupling terms. In the solid-state environment the exciton is coupled not only directly to the cavity mode, but also via the phonon bath.[37,38,70,78]

Upon increasing the pumping level, one reaches the nonlinear regime and climbs the Jaynes-Cummings ladder.[28] For the cavity emission at resonance, in a typical system where the coupling strength is not much larger than the decay rates, this transition results in an apparent collapse of the Rabi doublet into a single line. If the number of photons is high enough, this line narrows as a consequence of the cavity entering the lasing regime.[79] This transition, displayed as a solid (blue) curve in Fig. 3, has been reported experimentally.[17] Its counterpart in the dot emission [dotted (purple) line] is richer in qualitative features in the nonlinear regime.[28] This manifests by the elbows in Figs. 3(b)–3(d) [indicated by arrows in Fig. 3(b)] that arise from the transitions $|n,\pm\rangle \rightarrow |n-1,\mp\rangle$, which are suppressed in the cavity emission. We have used the standard notation for the eigenstates of the Jaynes-Cummings Hamiltonian with $|n,\pm\rangle$ the state with n excitation(s) of higher (+) and lower (−) energy (the level structure is displayed in Fig. 2 of Part II). In the lasing regime, Fig. 3(d), the dot emission is strongly non-Lorentzian and exhibits a characteristic line shape reminiscent of the one-atom laser.[79]

A simple and convenient way to evidence Jaynes-Cummings nonlinearities is to bring the system out of resonance. In this way, transitions that are otherwise closely packed together can be separated and resolved in the photoluminescence spectrum. This is shown in Fig. 4 for the same system as previously but detuning the two bare emitters from each other by $\Delta = \omega_1 - \omega_a$. The Rabi doublet at resonance turns into a triplet at small detunings. This is because one of the transitions, $|2,\pm\rangle \rightarrow |1,\pm\rangle$—which is too broad and too close to the linear transitions $|1,\pm\rangle \rightarrow |\text{vacuum}\rangle$ at resonance—can be distinguished at a small detuning, as shown in Figs. 4(a) and 4(b).

Transitions between dressed states provide a faithful mapping to the exact system dynamics when the system operates in the very strong coupling regime, such that dressed states are well defined and do not overlap appreciably with each other. In the case where they overlap, say because the splitting between dressed states is small or because their broadening is large, interferences between the states enter the picture. The luminescence can indeed be decomposed as a sum of Lorentzian emissions from the dressed states with dispersive corrections arising from each dressed state driving or being driven by the others.[28] These interferences can become particularly strong and complex when the system is brought toward the classical regime, that is, with a lot of excitations. In this case, many dressed states enter the collective dynamics, and their overlap as well as mutual disturbance are thus much stronger. This effect is also better seen at nonzero detuning. Although the interference grows with pumping also at resonance, it tends to be canceled by symmetry: dressed states from both sides of the origin (set at the bare cavity emission) equilibrate each other. However, with detuning, imbalance between emission from various dressed states magnifies the interferences. This is shown for instance in Fig. 5, which reproduces Fig. 3 (for the dot emission only) but at detuning $\Delta = 2g$. The figure shows how, as pumping

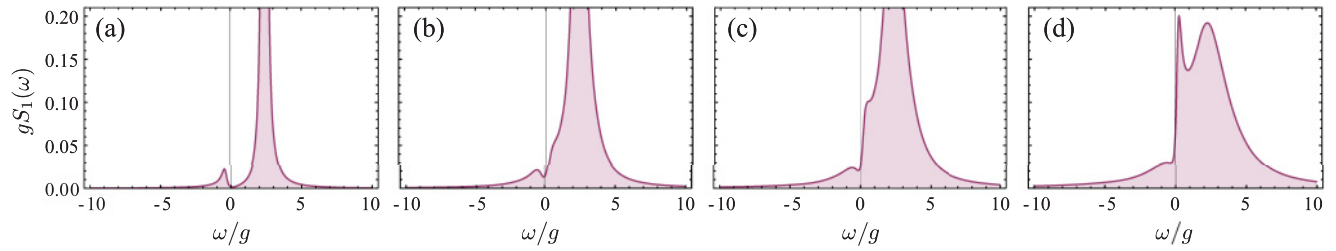

FIG. 5. (Color online) Dot emission spectrum of one dot in a cavity, out of resonance, as a function of pumping. The Rabi doublet in the spontaneous emission regime (a) gives rise, with increasing pumping (b)–(d), to an emission dip: the incoherent excitation is coherently scattered to the cavity which enters the lasing regime. This is better seen at nonzero detuning. Parameters are the same as in Fig. 3 but for $\Delta = 2g$.

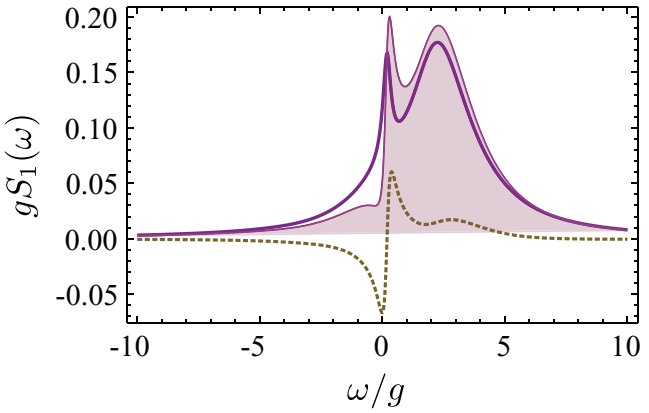

FIG. 6. (Color online) Detail of Fig. 5(d). The interference that arises as the system enters lasing is best seen in the detuned system because dressed states [solid (purple) curve] are then of a markedly different character; cf. the exciton line broadened by pumping (on the right), and the narrow line of the cavity that enters lasing (at the origin). The interferences between dressed states [dotted (brown) curve], which added to the dressed state emission provide the photoluminescence spectrum [filled (purple) area], strongly modify the results of kinetic theory applied to the dressed states.

is increased, an "emission dip" develops at the origin as the lines broaden (we use this terminology of a "dip" from the mere appearance it takes in the spectral shape). It starts to be particularly visible in Fig. 5(b), whereas, at low excitation [Fig. 5(a)], one merely sees the exciton, detuned, favoring its own mode of radiation, just as in the linear case (cf. Fig. 2). Note how, at resonance, in Fig. 3, this interference is masked, being essentially canceled by symmetry.

The physical origin of this dip is linked to the cavity entering the lasing regime at this frequency and, therefore, depleting excitation from the quantum dot.[80] In Fig. 6, we show a decomposition of Fig. 5(d) into the sum of dressed-state emission [thick solid (purple) curve] and the sum of interferences between the dressed states [dashed (brown) curve]. The observed photoluminescence spectrum is the sum of these two contributions, obtained from a mathematical decomposition of $G^{(1)}(t,\tau) = \langle a^\dagger(t)a(t+\tau)\rangle$ into terms that give rise to Lorentzian lines (identifying the dressed states) and to dispersive interferences when the dressed-state emissions overlap.[28] The final result can be adequately described by the dressed states only whenever interferences between them are negligible, that is, when they do not overlap. This is the case at low excitation and in the very strong coupling regime, when $g \gg \gamma_a, \gamma_1$ and the splitting-to-broadening ratio of all transitions is large. In this case, a kinetic theory that computes mean occupation of the dressed states with rate (Boltzmann) equations is adequate.[40] Otherwise, a full master equation approach is required, although it may quickly become intractable numerically. As the intensity is further increased, interferences result in the breakdown of the dressed-state picture when the system acquires some macroscopic coherence. Analytical investigations show that the emission dip corresponds to a coherent scattering peak from the dot to the cavity, which, in some approximations, becomes a Dirac δ function that describes Rayleigh scattering.[79] We will now see how such phenomena can be magnified in the case of N emitters and transported to the cavity emission, which is easily detectable.

IV. MORE THAN ONE EMITTER

The dynamics of systems containing several strongly coupled and strongly dissipative emitters becomes extremely interesting and rich as new paths of coherence flow between the dressed states are opened by pumping and decay. This can give rise to new peaks not accounted for by the dressed-state picture.[81]

At low pumping, when all N-QD excitons are exactly at resonance with the cavity mode, the eigenvalues and eigenstates of the system (neglecting incoherent loss, and setting the origin of the energy scale to ω_a) have a simple and well-known form:[82] two are split in energy by $\lambda_{\substack{N\\0}} = \pm\Omega$, where $\Omega = \sqrt{\sum_{j=1}^{N} g_j^2}$, while the other $N-1$ are degenerated and equal to 0. The corresponding eigenstates are

$$|\lambda_{\substack{N\\0}}\rangle = \frac{1}{\sqrt{2}}\left(\sum_{j=1}^{N}\frac{g_j}{\Omega}|0,X_j\rangle \pm |1,0\rangle\right), \tag{6a}$$

$$|\lambda_{j-1}\rangle = \frac{1}{\Omega_j}(g_1|0,X_j\rangle - g_j|0,X_1\rangle), \tag{6b}$$

with $\Omega_j = \sqrt{g_1^2 + g_j^2}$, with j ranging from 2 to N for the degenerate eigenstates in Eq. (6b). From this solution we can see that only the $|\lambda_{\substack{N\\0}}\rangle$ states have a contribution from the cavity photons. The cavity mode does not contribute to the other states $|\lambda_{j-1}\rangle$, which are called, for this reason, *dark states*. They consequently cannot be probed in the cavity spectrum $S_a(\omega)$, but they can be very well seen in the excitonic radiation channel or in a mixture of all radiation channels. These superpositions also give rise to the phenomena of sub- and superradiance, first reported by Dicke.[83] This is essentially a classical effect that is also observed with vibrating strings. Recently, such configurations have been analyzed in the microcavity QED context by Temnov and Woggon[84] and Auffèves *et al.*,[47] who studied the photon statistics, and by Poddubny *et al.*,[40] who studied the photoluminescence line shapes. The latter authors found that this classical regime is particularly fragile with regard to incoherent pumping since dark states, being also excited by pumping, act as a long-lived reservoir for bright states from higher manifolds. They also analyzed the regime of very high excitations, when the system is (or is going toward) lasing. They observe in such a case that, due to the predominance of the Dicke states that are the most highly degenerated, the cavity spectrum is either oddly or evenly peaked depending on the parity of the number of strongly coupled dots, which is a strong manifestation in a readily measured observable of the underlying microscopic configuration. The former authors also report oscillations in the statistics with parity of the number of emitters. In the following, we address particular cases of larger than one, but still small numbers of dots, and show how, in the linear regime, photoluminescence spectra vary greatly in a qualitative way because of the contribution or suppression of the dark states. We confirm that these states are quickly spoiled with

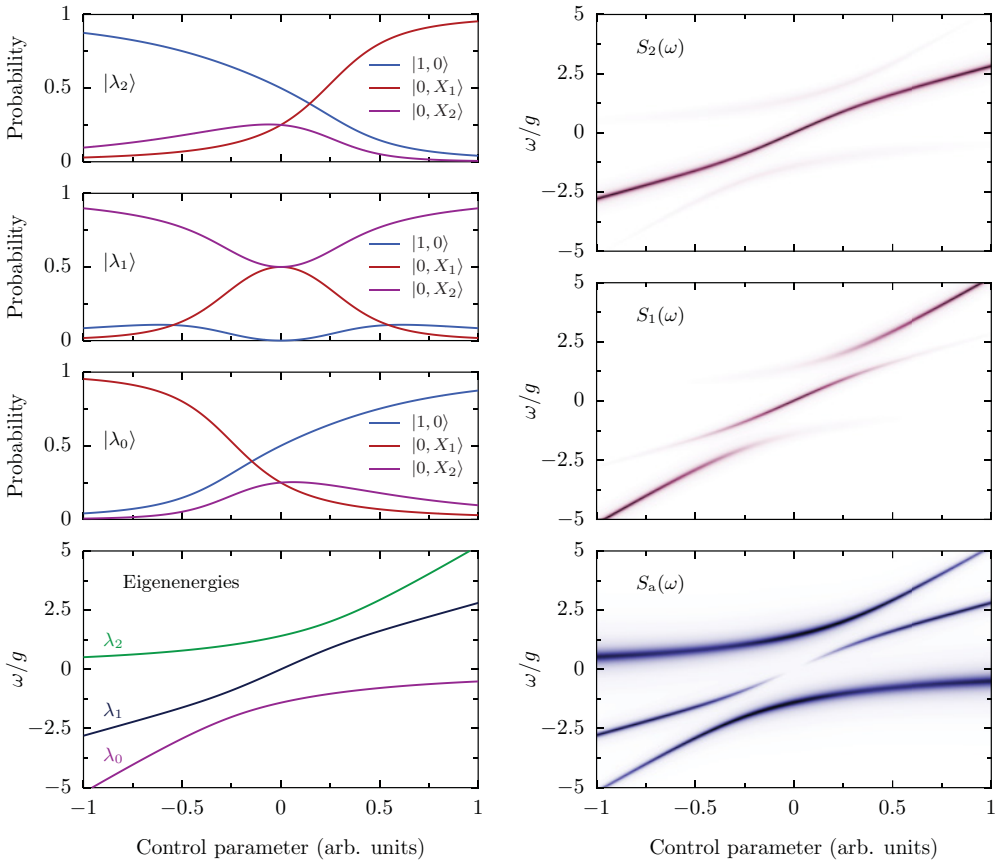

FIG. 7. (Color online) Emission spectrum from the radiation channel of the first exciton $S_1(\omega)$, the second exciton $S_2(\omega)$, the cavity mode $S_a(\omega)$, and the eigenstates for a strongly coupled system of two excitons and the cavity mode. The eigenvectors of the three eigenstates $|\lambda_2\rangle$, $|\lambda_1\rangle$, and $|\lambda_0\rangle$ of the coupled system display the contributions of the individual quantum states $|1,0\rangle$, $|0,X_1\rangle$, and $|0,X_2\rangle$ to the specific eigenstate. Parameters: same as in Fig. 2 with identical pumping of the dots.

increasing pumping[40] and show that they give rise to nonlinear quantum features, which also manifest in strikingly different ways depending on the radiation channel that is probed.

A. Two emitters

In the case of two emitters coupled to a single cavity mode, the eigenfrequencies in the linear regime can be obtained by solving the eigenvalue problem given by the following equation:

$$i\frac{\partial}{\partial t}\begin{pmatrix}\langle a\rangle\\ \langle\sigma_-^1\rangle\\ \langle\sigma_-^2\rangle\end{pmatrix}=\begin{pmatrix}\tilde{\omega}_a & g_1 & g_2\\ g_1 & \tilde{\omega}_1 & 0\\ g_2 & 0 & \tilde{\omega}_2\end{pmatrix}\begin{pmatrix}\langle a\rangle\\ \langle\sigma_-^1\rangle\\ \langle\sigma_-^2\rangle\end{pmatrix}, \qquad (7)$$

where $\tilde{\omega}_a=\omega_a-i\Gamma_a/2$ and $\tilde{\omega}_j=\omega_j-i\Gamma_j/2$, with $\Gamma_a=\gamma_a-P_a$, and $\Gamma_j=\gamma_j+P_j$. From the eigenstate of the emission eigenfrequency we can obtain the degree of mixture of each peak in the spectrum, i.e., the strength of the contribution of the cavity mode, QD1 exciton and QD2 exciton, to each individual eigenstate.

In Fig. 7, we investigate a system of two excitons in different QDs simultaneously coupled to one cavity mode in the linear regime. We compare the emission spectra obtained via the radiation channel of the first exciton $S_1(\omega)$, the second exciton $S_2(\omega)$, and the cavity mode $S_a(\omega)$. In the spontaneous emission regime, while all three radiation channels exhibit a markedly different emission spectrum, the most striking difference can be found in $S_a(\omega)$, where one of the emission lines vanishes completely. This occurs when subradiance sets in, and it follows for the case of two emitters from an analysis of the eigenvectors similar to that of Ref. 19. The plot of the eigenvectors in Fig. 7 presents the contributions of the three quantum states $|1,0\rangle$, $|0,X_1\rangle$, and $|0,X_2\rangle$ to the three eigenstates $|\lambda_2\rangle$, $|\lambda_1\rangle$, and $|\lambda_0\rangle$ (as marked in the plot of the eigenstates) of the coupled system. While $|\lambda_2\rangle$ and $|\lambda_0\rangle$ have contributions from all three quantum states at resonance, for the eigenstate $|\lambda_1\rangle$ the contribution from $|1,0\rangle$ goes to zero due to destructive interference.

A measurement of this kind would also be possible for the system just described, but when the two exciton lines anticross out of resonance from the cavity mode, similar to that discussed in Ref. 19. In Fig. 8, we plot the emission spectrum from the radiation channel of the cavity mode $S_a(\omega)$, and the eigenstates of such a system. Probing the cavity emission, one of the emission lines vanishes, similar to the case in Fig. 7, but this time when the two excitons are crossing out of resonance from the cavity mode. In this situation the eigenvalues and eigenstates have also a simple form, $\lambda_1=\Delta$, $\lambda_{\frac{2}{0}}=\Delta/2\pm\sqrt{\Delta^2+4(g_1^2+g_2^2)}/2$, with $\Delta=\omega_1-\omega_a$ being the mutual detuning from the cavity mode. In this case, the

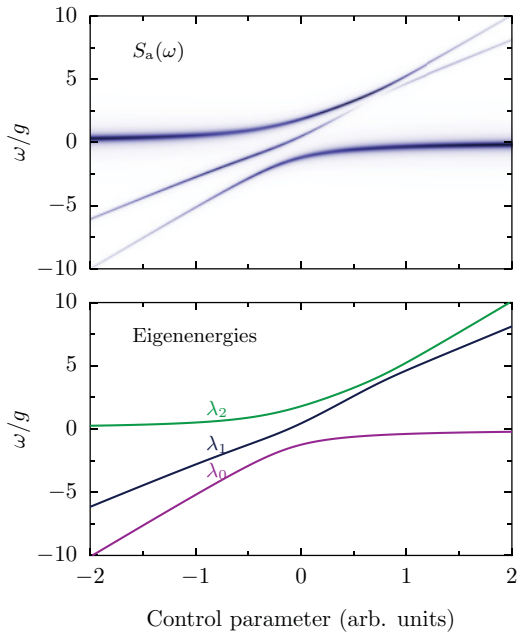

FIG. 8. (Color online) Emission spectrum from the radiation channel of the cavity mode $S_a(\omega)$, and eigenstates for a strongly coupled system of two excitons and the cavity mode where the two excitons cross out of resonance from the cavity mode. Parameters: same as in Fig. 7.

eigenstates are

$$|\lambda_{\frac{2}{0}}\rangle = \frac{1}{\sqrt{(\lambda_{\frac{2}{0}})^2 + \Omega_2^2}}\left(g_1|0,X_1\rangle + g_2|0,X_2\rangle - \lambda_{\frac{2}{0}}|1,0\rangle\right),$$

$$|\lambda_1\rangle = \frac{1}{\Omega_2}(g_1|0,X_2\rangle - g_2|0,X_1\rangle). \quad (8)$$

Again, since the contribution from the cavity mode to this particular eigenstate ($|\lambda_1\rangle$) goes to zero, it cannot be probed by the cavity radiation. The plot of all three eigenstates, however, clearly shows the anticrossing behavior of the two excitonlike states when they come into resonance detuned from the cavity mode.[19] The disappearance of the second peak during the anticrossing of the excitons brings a clear signature of a collective strong coupling with the two dots and that this is probed in the cavity radiation channel only. This phenomenon should also have been present in the experiment of Ref. 19, with a numerically extracted splitting of $\approx$10 μeV. However, due to experimental limitations (resolution of the monochromator $\Gamma_R = 18$ μeV) and high rates of dephasing ($\gamma_{QD}^{\phi} = 10$–20 μeV), neither the anticrossing of the two excitons nor the disappearance of the central peak were observable.

This interference in the linear regime persists in the nonlinear regime, where it turns into the interference related to coherence buildup in the system, as was the case with one dot in the cavity (cf. Figs. 5 and 6). Such interferences are, however, now directly accessible through the cavity spectrum, whereas they were previously only visible in the dot emission, which is technically more challenging. This is shown at resonance [Fig. 9(a)] and out of resonance [Figs. 9(b) and 9(c)]. The sharp line near the origin in Figs. 9(b) and 9(c) is the exciton line

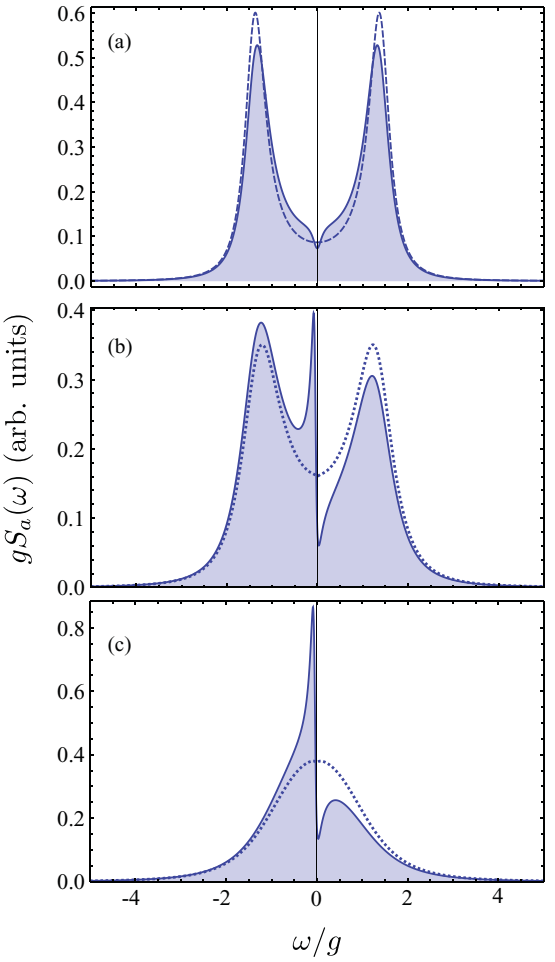

FIG. 9. (Color online) Spectral shapes in the cavity emission when two dots are strongly coupled to the cavity mode. (a) With increasing excitation (solid) the emission dip effect becomes visible in the cavity emission. (b) It is better seen slightly out of resonance since it can now "feed" on the line previously canceled by subradiance. (c) Such interferences are strong even in systems that do not exhibit spontaneous emission features (such as Rabi splitting), although this still requires strong coupling. Parameters: $g_1 = g_2 = g$ (setting the unit), $\gamma_a = g$, $\gamma_1 = \gamma_2 = 0.1g$, $P_a = 0$; then (a) $\Delta_1 = \Delta_2 = 0$, $P_1 = 10^{-4}g$ with (dashed) $P_2 = 10^{-4}g$ and (solid) $P_2 = 0.1g$. (b) Same as (a) but for $\gamma_a = 2g$, $P_1 = 10^{-3}g$, $P_2 = 0$, $\Delta_1 = 0$ and (solid) $\Delta_2 = 0.1g$ or (dotted) $\Delta_2 = 0$. (c) Same as (a) but for $\gamma_a = 5g$, $\Delta_1 = 0$ with (dotted) $\Delta_2 = 0$ or (solid) $\Delta_2 = 0.1g$.

that appears suddenly as subradiance cancellation is destroyed by going out of resonance; cf. Fig. 7. It results from the interplay of subradiance and detuning, studied in Ref. 32, and the method outlined there indeed reproduces such spectral features in the linear regime. In the nonlinear regime, this line also suffers from the dip carved by the cavity, where it is sharply located. This effect is robust regardless of the broadening of the cavity, i.e., with and without observation of the Rabi doublet. Here again, detuning is paramount in revealing the underlying physics, as seen in Figs. 9(b) and 9(c) where the resonant case is superimposed as a dotted line: a very small dip at $\omega = 0$ is hardly visible at resonance [similar

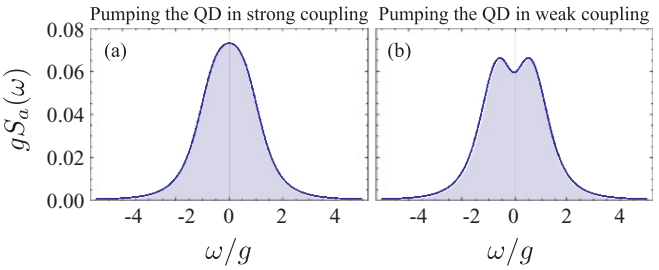

FIG. 10. (Color online) Luminescence spectra of the cavity in strong coupling with one QD and in weak coupling with another QD, in the cases where (a) the strongly coupled dot or (b) the weakly coupled dot is excited. In the latter case, the effective cavity pumping from the weakly coupled, or spectator, QD allows to resolve a line splitting, which would not be observed if there would be only one dot. Parameters: $\gamma_a = 3g, \gamma_1 = \gamma_2 = g, g_1 = g, g_2 = g/10$, $\Delta_1 = \Delta_2 = 0$, with $P = 0.2g$ on (a) the first or (b) the second dot.

to the solid line in Fig. 9(a)], in contrast to the detuned case that produces a significant discontinuity in the spectral shape.

The case of two emitters is also the simplest to illustrate a possible mechanism of cavity feeding, provided by a spectator dot which does not enter the strong-coupling dynamics but changes the effective quantum state of the system. In Fig. 10, we show the situation of two dots at resonance, in a system where one dot, say QD1, is in strong coupling, while the other dot, QD2, is in weak coupling. The cavity photoluminescence is shown in the cases where QD1 is pumped [Fig. 10(a)] or where QD2 is pumped [Fig. 10(b)]. In the former case, the direct excitation of the quantum dot makes the quantum state excitonlike and the Rabi splitting is not resolved. In the latter case, the excitation transits by the spectator dot that emits it by Purcell enhancement directly into the cavity, thus resulting in a photonlike quantum state. As a result, the splitting is resolved. The dynamics results in a photon fraction of $\approx 24\%$ when exciting directly the strongly coupled dot versus $\approx 66\%$ when exciting the spectator one. These values provide a line shape in good qualitative agreement with an effective cavity pumping.[23]

Well in the nonlinear regime, many dressed states are excited that reinforce or, on the contrary, destroy the effects just described. We show a few illustrative results, keeping in

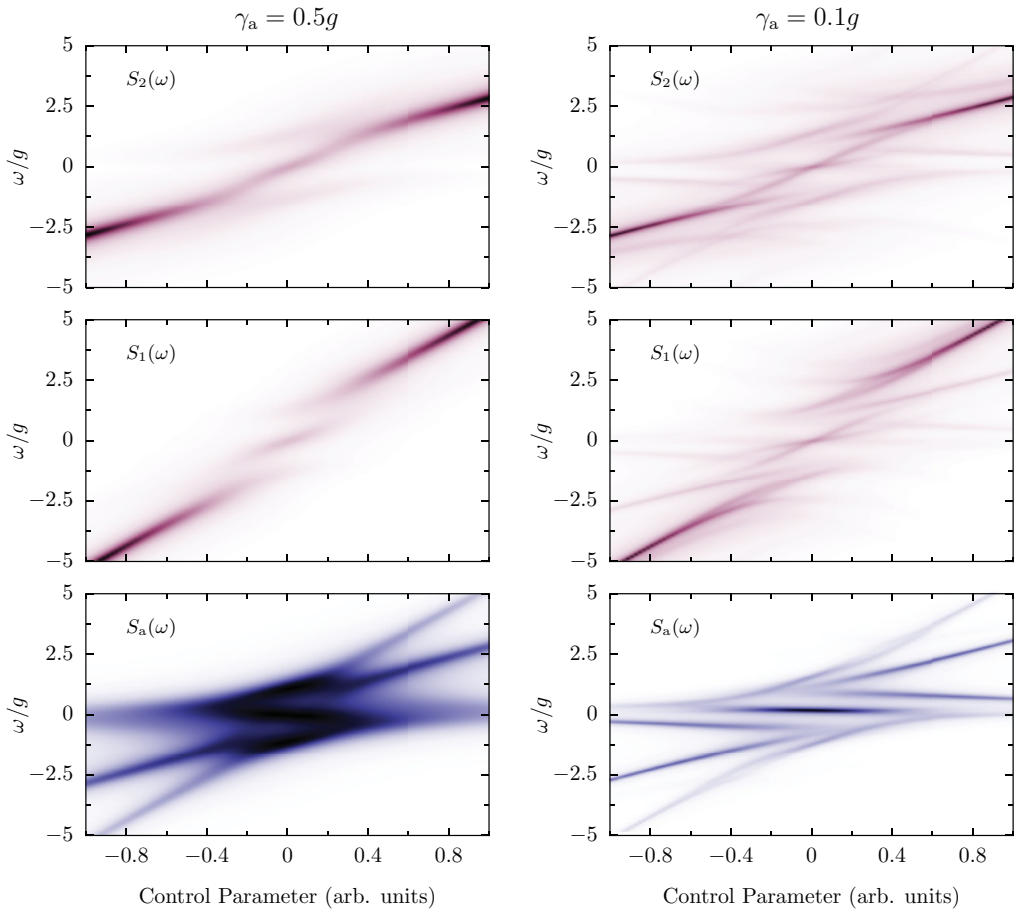

FIG. 11. (Color online) Emission spectrum from $N = 2$ dots in strong coupling with the cavity mode in the detuning configuration where the dots drift with slopes proportional to the control parameter in the ratios 1 and 1/2, respectively, both meeting the cavity at the same point. The left and right graphs, corresponding to standard and excellent strong coupling, respectively, are to be compared. The profusion of dressed states in the best system and the even greater number of possible transitions between them give rise to the crowded set of lines in the dot emission, featuring both crossing and anticrossing of the lines. The figure is also to be compared with Fig. 12 with a different detuning configuration, realizing in particular a qualitatively different profile of the cavity emission in the case $\gamma_a = 0.5g$.

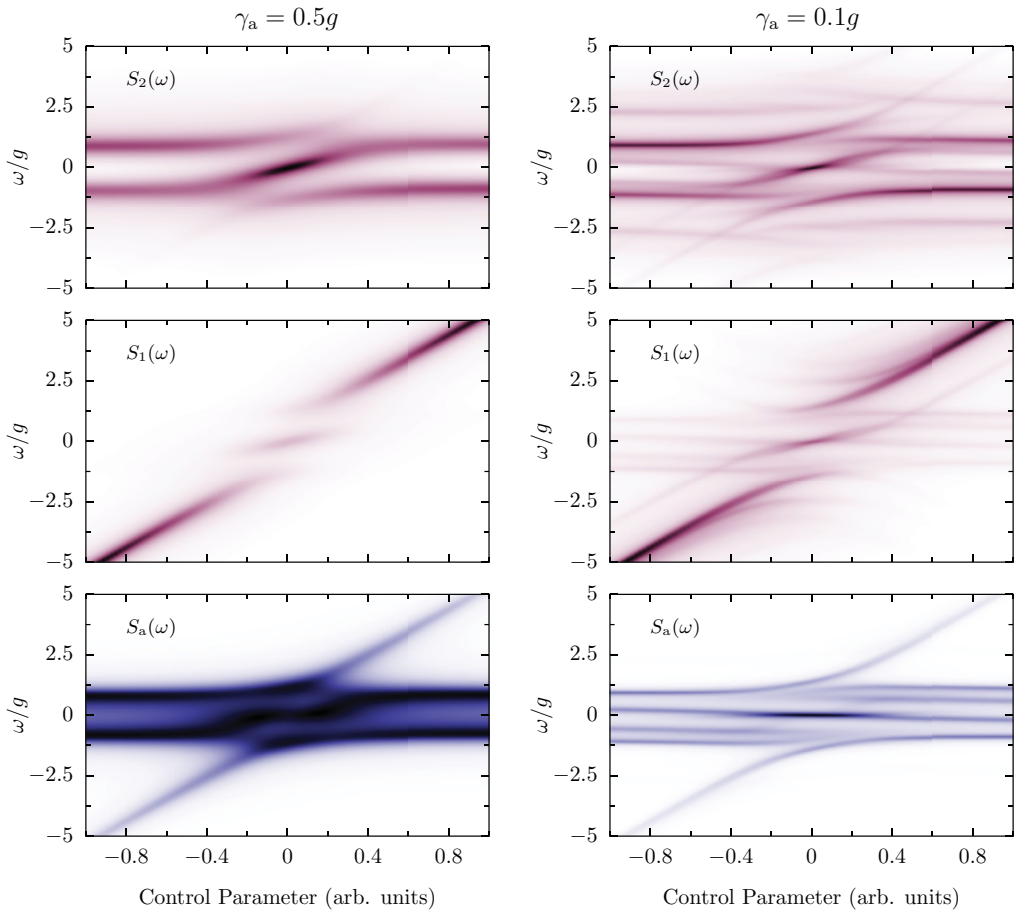

FIG. 12. (Color online) Same as Fig. 11 but for a different configuration of detuning, with one QD always at resonance and the other tuning through with slope proportional to the control parameter. The profile varies topologically in the cavity emission of the less strongly coupled system, which is the case of easiest experimental access.

mind that there is a wealth of other possible configurations that give rise to possibly greatly different results. To bring some perspective into which parameters affect more crucially the outputs, we compare both the case of various strengths of the coupling and the case of various detuning configurations. Namely, we compare the case of state-of-the-art cavities on the

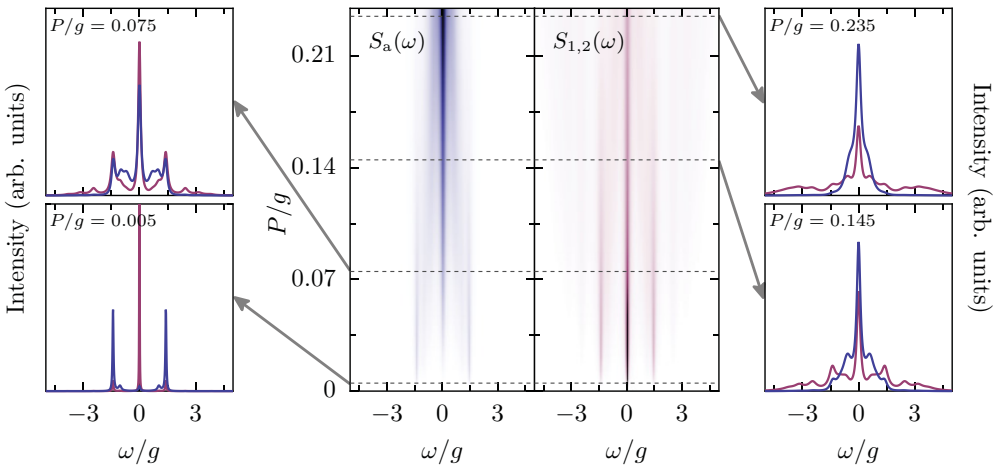

FIG. 13. (Color online) Emission spectra from $N = 2$ dots in strong coupling with the cavity mode in the case $\gamma_a = 0.1g$, at resonance and as a function of increasing pumping. The nonlinear regime breaks the subradiance in the cavity emission and the central peak appears, followed by quantum nonlinear features, and ultimately the system goes toward lasing, with characteristic features such as the emergence of a single narrowing line in the cavity emission and of an emerging Mollow triplet in the dot emission.

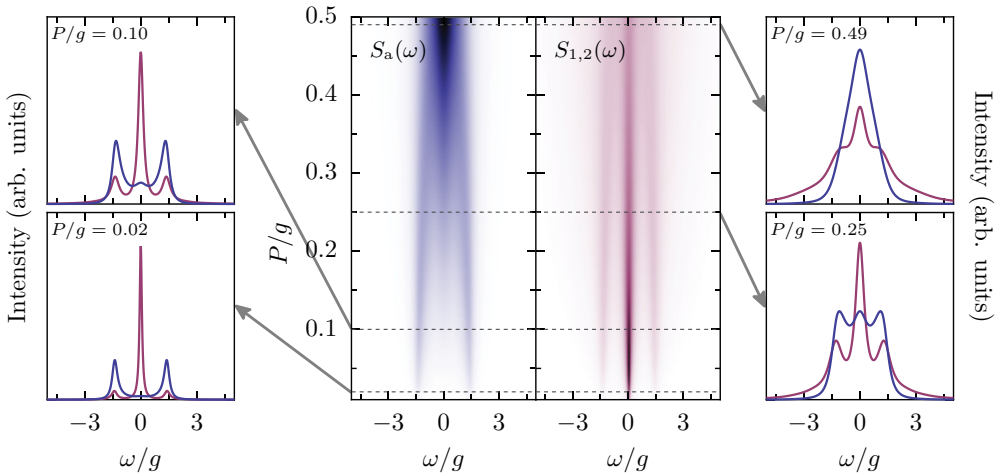

FIG. 14. (Color online) Same as Fig. 13 but for a lower Q system, with $\gamma_a = 0.5g$. Increasing pumping also breaks subradiance and lets the central peak appear in the cavity emission. In this case, however, quantized nonlinearities cannot be resolved and the system requires higher pumping to show signatures of lasing in the cavity emission. The transition is therefore merely that from a doublet to a triplet that ultimately collapses to a single line in the cavity, and of a singlet to a triplet in the dot emission.

one hand, with $\gamma_a = 0.5g$, and of very high Q cavities on the other hand, with $\gamma_a = 0.1g$. The latter enables us to see clearly the various transitions in a system where dressed states are well defined in isolation, while the former shows how their interferences contrive to alter this picture in a less good, but also more realistic system. For anticrossing results, we consider two configurations of detunings, again to be compared between each other. These are displayed in Figs. 11 and 12. In the first case, the two quantum dots drift along a different slope with the control parameter. In the second case, only one dot drifts while the other one stays pinned at resonance with the cavity. The spectra at resonance (when the control parameter is zero) are therefore the same in Figs. 11 and 12. The overall density plot, however, displays qualitatively different behaviors with small detuning, when γ_a is not very small (left column). In one case (Fig. 11), the conventional anticrossing scenario of Fig. 2 is essentially reproduced with two dots that approach the cavity and give rise to level repulsion in the presence of the cavity mode. In the other case (Fig. 12), the Rabi doublet stays robust as the dot approaches and gets transferred on the side opposing the drifting dot as it gets in resonance. The two configurations vary in a qualitative way since the connections between the three lines far from resonance are topologically different. There are two pairs of meeting points in Fig. 11, where the line shape becomes a doublet, while there are none in Fig. 12, where the central line remains sandwiched between the outer lines, with which it exhibits an anticrossing. Other detuning configurations give rise to variations on these themes. The QD emission, which proved more rich in features that evidence quantum nonlinearities with one QD, is, however, with $N = 2$, more uniform in its phenomenology, exhibiting less variety of shapes and patterns beyond different weighting of the lines. In particular, the anticrossing pattern is closer to that of the linear regime. When γ_a is very small (right column), the luminescence becomes extremely complicated and overcrowded with lines in the dot emission, stemming from all the possible transitions between the dressed states that are all allowed, as in the case of one QD. In the cavity emission, however, the cavity selection rules result in a much neater luminescence profile that, when dressed states do not interfere significantly, turns out to be quite similar regardless of the detuning configuration.

Back to resonance, we now link the two limiting cases just described, going from the linear to the nonlinear regime, by considering luminescence in both channels of emission as a function of increasing pumping. This is shown in Figs. 13 and

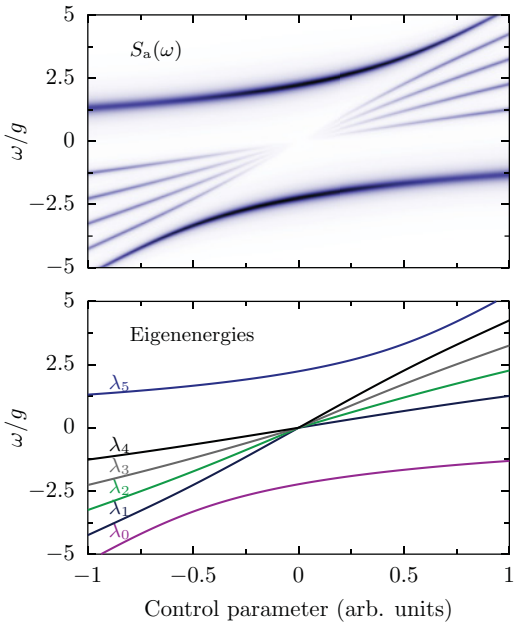

FIG. 15. (Color online) Emission spectrum from the radiation channel of the cavity mode $S_a(\omega)$ and the eigenstates of a strongly coupled system with $N = 5$ QDs. Parameters are the same as in Fig. 7.

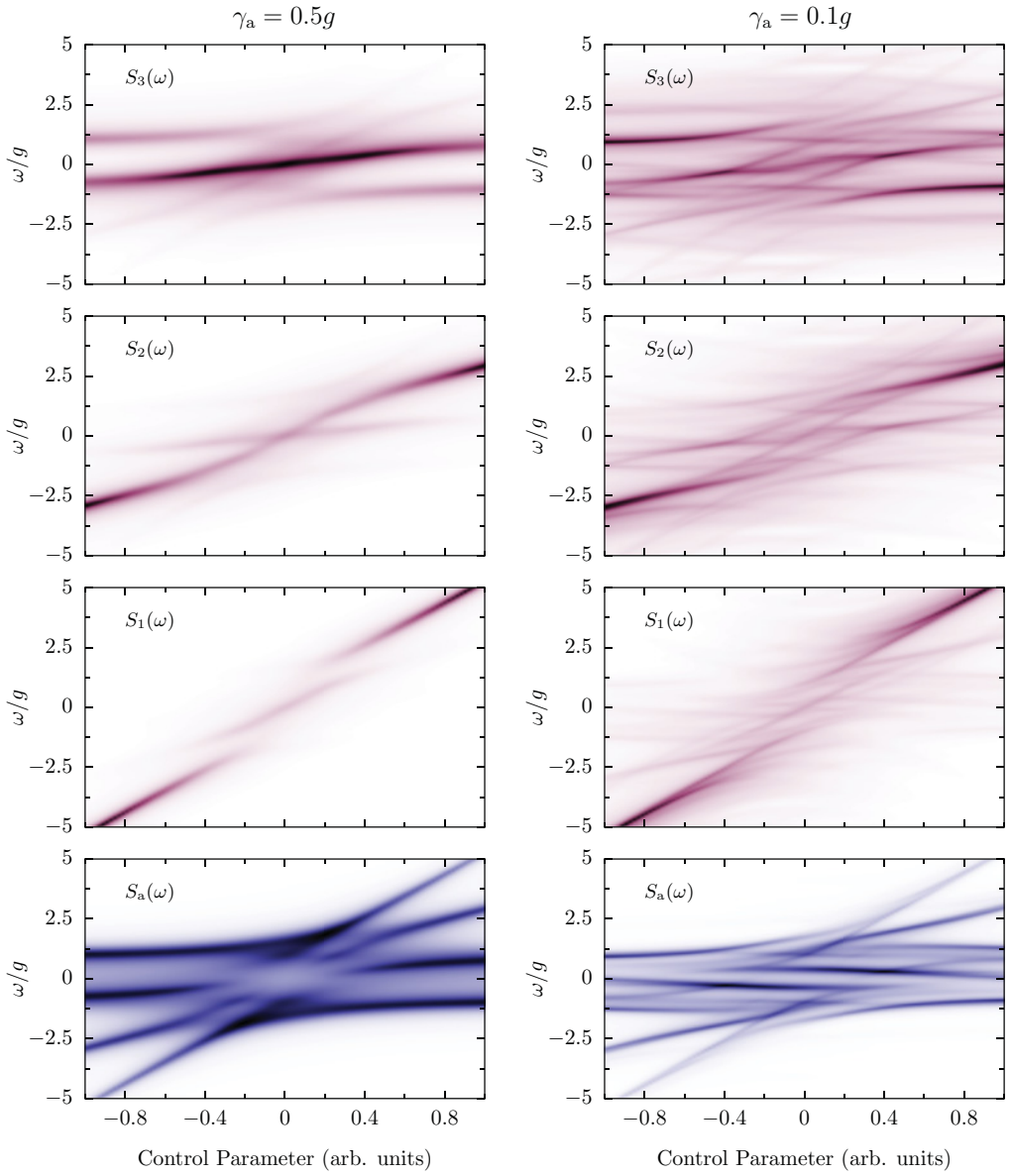

FIG. 16. (Color online) Counterpart for $N = 3$ of Fig. 11, with two dots drifting with slopes in the ratio 1 and 1/2 and a third dot pinned at resonance. The cavity emission displays both features of peak cancellation and quantum nonlinearities in the case $\gamma_a/g = 0.5$, and a complex profile of crossing and anticrossing lines in the case $\gamma_a/g = 0.1$, akin to dot emission with $N = 2$. The dot emission becomes so crowded as to lose any recognizable pattern, already for N as low as three.

14, again for the cases $\gamma_a/g = 0.1$ and 0.5, respectively. In both cases, one can see the transition from the linear to the quantum nonlinear regime, with peak cancellation as a result of the subradiance effect. Figure 14, for instance, shows the neat evolution of the Rabi doublet into a spectral triplet. In the better system, Fig. 13, the same transition is seen but now also featuring explicitly various transitions between higher excited dressed states, thus showing the simultaneous and separate appearance of the subradiant state and of quantum nonlinear transitions. Note that, as compared to the case of one emitter, the cavity emission may display a rich structure, in some cases equally rich or richer than the quantum dot emission. Finally, in this case, with increasing pumping, the system undergoes lasing and in the dot emission an emergent two-atom Mollow triplet starts to form.

B. Three emitters and beyond

One can continue the exhibits for increasing values of N, and we now do so for the case $N = 3$ or, in the linear regime, $N = 5$, as in this latter case the phenomenology is easily generalized to arbitrary values. In the linear regime, indeed, the interference in the cavity emission due to settling of dark states simply scales in the expected way with the number of dots: as many lines vanish as there are corresponding strongly coupled dots (minus one). As an example, we simulate the spectral

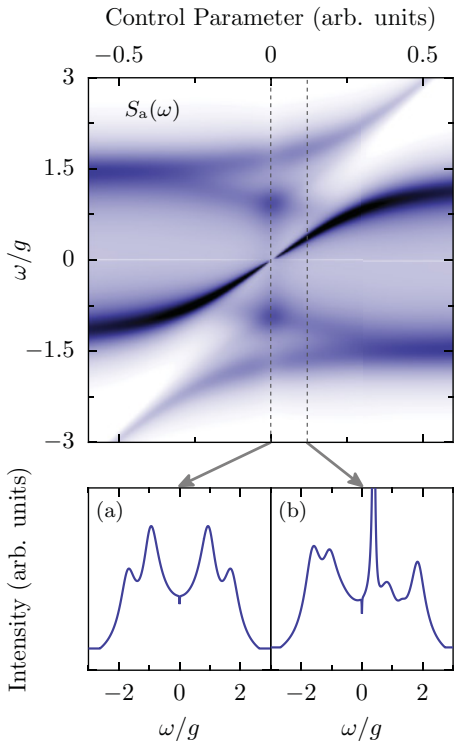

FIG. 17. (Color online) Cavity emission when three dots are strongly coupled to the cavity mode at low pumping with (a) resonance and (b) one case out of resonance shown explicitly. This case brings together most features described above: the Dicke nonlinearities (here with $N = 3$), the subradiance with disappearance of the sharp central line at resonance, and the emission dip at the cavity mode. Note how the last feature results in the sharp horizontal line in the density plot.

shapes of a system of five identical quantum emitters coupled to the same cavity mode and we plot in Fig. 15 the emission spectrum from the radiation channel of the cavity mode $S_a(\omega)$ and the corresponding eigenvalues. At resonance, the cavity radiation channel shows only the anticrossing of two of the eigenstates of the coupled system, albeit with a larger splitting corresponding to 2Ω, as described before in Eq. (6a). In the quantum nonlinear regime, however, the number of possible transitions quickly renders the output hopelessly complex in its specifics, while the main qualitative results remain essentially the same as for $N = 2$, but now set in an even more crowded environment. In Fig. 16, for instance, we reproduce the case of Fig. 11 but with three dots. The parity effect results in an even and symmetric distribution of peaks at resonance. In the best system (right column), the cavity emission shows once more that the features of the dot emission of cases with lower N, namely the photoluminescence lines, previously neatly packed together and ordered, start to display the chaotic features of disordered superpositions with both crossing and anticrossing. We conclude with another variation of the $N = 3$ case, shown in Fig. 17, that dramatically brings together the two types of strong interferences that manifest themselves in this system: subradiance and the emission dip. This time, two dots stay pinned at resonance while the third one is tuned through, and we display the cavity emission with two sections at resonance [Fig. 17(a)] and slightly out of resonance [Fig. 17(b)] for the case $\gamma_a = g$. In both cases the emission dip is seen at $\omega = 0$ (in the form of a white horizontal line in the density plot). The Rabi doublet, now at $\pm\sqrt{3}g$, is visible but is dominated by transitions of multiply excited states, so we are clearly far from the linear regime. Subradiance is however robust, and a small detuning breaks it just like in the linear case, resulting in the dot eigenstate suddenly showing up as a very sharp and strong peak that actually dominates most of the density plot profile. These features are magnified by an asymmetry in the pumping rates, namely $P_2 = 10^{-2}g$ and $P_1 = P_3 = 0$. These results show again how the main trends can take on varying forms depending on the specific parameters.

V. CONCLUSIONS

We investigated theoretically the spectral shape of the emission from N QDs strongly coupled to a single mode of a microcavity. The emission spectra obtained from the two different radiation channels offered by the cavity and direct quantum dot emission were compared, both in the linear and nonlinear regime, in and out of resonance. In the spontaneous emission regime, dark states forming at resonance result in a vanishing of spectral lines in the cavity emission only. As the level of excitation is increased and multiple-photon effects become important, dressed states enter the picture. These are difficult to observe in state-of-the-art experiments where the splitting-to-broadening ratio does not allow them to be clearly resolved. Although strong coupling is maximum at resonance, we find that the study of detuned systems can provide a route to reveal the quantum nonlinear features. Moreover, here too dot emission behaves qualitatively differently from cavity emission. As excitation is further increased and a large number of cavity photons is generated (the system enters lasing), another interference due to onset of coherence takes place. This manifests itself as an emission dip that results from coherent and elastic scattering between the modes. In some cases, many of these effects can be seen together. A plethora of phenomena thus remain to be observed in these systems. One can access it either by detecting direct dot emission—which is technically difficult—or by considering strong coupling involving more than one emitter. In both cases, detuning is a powerful tool to unravel this new physics, since, although optimal, strong coupling is balanced and/or hidden at resonance.

ACKNOWLEDGMENTS

We thank Norman Hauke, Dr. Alexander Poddubny, and Dr. Mikhail Glazov for fruitful discussions. We acknowledge financial support of the DFG via the SFB 631, the German Excellence Initiative via NIM, and the EU-FP7 via SOLID. J.M.V.B. acknowledges the support of the Alexander von Humboldt Foundation, CAPES, CNPQ, and FAPEMIG; E.d.V. acknowledges support of a Newton International fellowship, the Emmy Noether Project No. HA 5593/1-1 (DFG), and the Alexander von Humboldt Foundation; and F.P.L. acknowledges the support of the FP7-PEOPLE-2009-IEF project SQOD.

*fabrice.laussy@gmail.com

[1] T. Yoshie, A. Scherer, J. Heindrickson, G. Khitrova, H. M. Gibbs, G. Rupper, C. Ell, O. B. Shchekin, and D. G. Deppe, Nature (London) **432**, 200 (2004).

[2] J. P. Reithmaier, G. Sek, A. Löffler, C. Hofmann, S. Kuhn, S. Reitzenstein, L. V. Keldysh, V. D. Kulakovskii, T. L. Reinecker, and A. Forchel, Nature (London) **432**, 197 (2004).

[3] E. Peter, P. Senellart, D. Martrou, A. Lemaître, J. Hours, J. M. Gérard, and J. Bloch, Phys. Rev. Lett. **95**, 067401 (2005).

[4] S. Reitzenstein, A. Löffler, C. Hofmann, A. Kubanek, M. Kamp, J. P. Reithmaier, A. Forchel, V. D. Kulakovskii, L. V. Keldysh, I. V. Ponomarev, and T. L. Reinecke, Opt. Lett. **31**, 1738 (2006).

[5] K. Hennessy, A. Badolato, M. Winger, D. Gerace, M. Atature, S. Gulde, S. Fält, E. L. Hu, and A. Imamoğlu, Nature (London) **445**, 896 (2007).

[6] D. Englund, A. Faraon, I. Fushman, N. Stoltz, P. Petroff, and J. Vučković, Nature (London) **450**, 857 (2007).

[7] A. Faraon, I. Fushman, D. Englund, N. Stoltz, P. Petroff, and J. Vuckovic, Nat. Phys. **4**, 859 (2008).

[8] C. Kistner, T. Heindel, C. Schneider, A. Rahimi-Iman, S. Reitzenstein, S. Höfling, and A. Forchel, Opt. Express **16**, 15006 (2008).

[9] M. Winger, A. Badolato, K. J. Hennessy, E. L. Hu, and A. Imamoğlu, Phys. Rev. Lett. **101**, 226808 (2008).

[10] A. Laucht, F. Hofbauer, N. Hauke, J. Angele, S. Stobbe, M. Kaniber, G. Böhm, P. Lodahl, M.-C. Amann, and J. J. Finley, New J. Phys. **11**, 023034 (2009).

[11] A. Laucht, N. Hauke, J. M. Villas-Bôas, F. Hofbauer, M. Kaniber, G. Böhm, and J. J. Finley, Phys. Rev. Lett. **103**, 087405 (2009).

[12] S. Münch, S. Reitzenstein, P. Franeck, A. Löffler, T. Heindel, S. Höfling, L. Worschech, and A. Forchel, Opt. Express **17**, 12821 (2009).

[13] S. Reitzenstein, S. Münch, P. Franeck, A. Rahimi-Iman, A. Löffler, S. Höfling, L. Worschech, and A. Forchel, Phys. Rev. Lett. **103**, 127401 (2009).

[14] Y. Ota, M. Shirane, M. Nomura, N. Kumagai, S. Ishida, S. Iwamoto, S. Yorozu, and Y. Arakawa, Appl. Phys. Lett. **94**, 033102 (2009).

[15] J. Suffczyński, A. Dousse, K. Gauthron, A. Lemaître, I. Sagnes, L. Lanco, J. Bloch, P. Voisin, and P. Senellart, Phys. Rev. Lett. **103**, 027401 (2009).

[16] S. M. Thon, M. T. Rakher, H. Kim, J. Gudat, W. T. M. Irvine, P. M. Petroff, and D. Bouwmeester, Appl. Phys. Lett. **94**, 111115 (2009).

[17] M. Nomura, N. Kumagai, S. Iwamoto, Y. Ota, and Y. Arakawa, Nat. Phys. **6**, 279 (2010).

[18] J. Kasprzak, S. Reitzenstein, E. A. Muljarov, C. Kistner, C. Schneider, M. Strauss, S. Höfling, A. Forchel, and W. Langbein, Nat. Mater. **9**, 304 (2010).

[19] A. Laucht, J. M. Villas-Bôas, S. Stobbe, N. Hauke, F. Hofbauer, G. Böhm, P. Lodahl, M.-C. Amann, M. Kaniber, and J. J. Finley, Phys. Rev. B **82**, 075305 (2010).

[20] D. Dalacu, K. Mnaymneh, V. Sazonova, P. J. Poole, G. C. Aers, J. Lapointe, R. Cheriton, A. J. SpringThorpe, and R. Williams, Phys. Rev. B **82**, 033301 (2010).

[21] L. C. Andreani, G. Panzarini, and J.-M. Gérard, Phys. Rev. B **60**, 13276 (1999).

[22] G. Cui and M. G. Raymer, Phys. Rev. A **73**, 053807 (2006).

[23] F. P. Laussy, E. del Valle, and C. Tejedor, Phys. Rev. Lett. **101**, 083601 (2008).

[24] J. I. Inoue, T. Ochiai, and K. Sakoda, Phys. Rev. A **77**, 015806 (2008).

[25] A. Naesby, T. Suhr, P. T. Kristensen, and J. Mork, Phys. Rev. A **78**, 045802 (2008).

[26] A. Auffèves, B. Besga, J.-M. Gérard, and J.-P. Poizat, Phys. Rev. A **77**, 063833 (2008).

[27] F. P. Laussy, E. del Valle, and C. Tejedor, Phys. Rev. B **79**, 235325 (2009).

[28] E. del Valle, F. P. Laussy, and C. Tejedor, Phys. Rev. B **79**, 235326 (2009).

[29] M. Yamaguchi, T. Asano, K. Kojima, and S. Noda, Phys. Rev. B **80**, 155326 (2009).

[30] S. Hughes and P. Yao, Opt. Express **17**, 3322 (2009).

[31] A. Auffèves, J.-M. Gérard, and J.-P. Poizat, Phys. Rev. A **79**, 053838 (2009).

[32] N. S. Averkiev, M. M. Glazov, and A. N. Poddubny, JETP **108**, 836 (2009).

[33] M. Richter, A. Carmele, A. Sitek, and A. Knorr, Phys. Rev. Lett. **103**, 087407 (2009).

[34] C. A. Vera, H. Vinck-Posada, and A. González, Phys. Rev. B **80**, 125302 (2009).

[35] C. A. Vera, A. Cabo, and A. González, Phys. Rev. Lett. **102**, 126404 (2009).

[36] G. Tarel and V. Savona, Phys. Rev. B **81**, 075305 (2010).

[37] P. Kaer, T. R. Nielsen, P. Lodahl, A.-P. Jauho, and J. Mørk, Phys. Rev. Lett. **104**, 157401 (2010).

[38] U. Hohenester, Phys. Rev. B **81**, 155303 (2010).

[39] S. Ritter, P. Gartner, C. Gies, and F. Jahnke, Opt. Express **18**, 9909 (2010).

[40] A. N. Poddubny, M. M. Glazov, and N. S. Averkiev, Phys. Rev. B **82**, 205330 (2010).

[41] G. Yeoman and G. M. Meyer, Phys. Rev. A **58**, 2518 (1998).

[42] S. Strauf, K. Hennessy, M. T. Rakher, Y. S. Choi, A. Badolato, L. C. Andreani, E. L. Hu, P. M. Petroff, and D. Bouwmeester, Phys. Rev. Lett. **96**, 127404 (2006).

[43] E. del Valle, F. P. Laussy, F. Troiani, and C. Tejedor, Phys. Rev. B **76**, 235317 (2007).

[44] C. A. Vera, N. Q. M, H. Vinck-Posada, and B. A. Rodríguez, J. Phys. Condens. Matter **21**, 395603 (2009).

[45] E. del Valle, e-print arXiv:1007.1784 (unpublished).

[46] P. C. Cárdenas, N. Quesada, H. Vinck-Posada, and B. A. Rodríguez, J. Phys. Condens. Matter **23**, 265304 (2011).

[47] A. Auffèves, D. Gerace, S. Portolan, A. Drezet, and M. F. Santos, New J. Phys. **13**, 093020 (2011).

[48] A. Wickenbrock, P. Phoonthong, and F. Renzoni, J. Mod. Opt. **58**, 1310 (2011).

[49] E. Gallardo, L. J. Martinez, A. K. Nowak, D. Sarkar, H. P. van der Meulen, J. M. Calleja, C. Tejedor, I. Prieto, D. Granados, A. G. Taboada, J. M. García, and P. A. Postigo, Phys. Rev. B **81**, 193301 (2010).

[50] H. Kim, D. Sridharan, T. C. Shen, G. S. Solomon, and E. Waks, Opt. Express **19**, 2589 (2011).

[51] S. Kiravittaya, A. Rastelli, and O. G. Schmidt, Rep. Prog. Phys. **72**, 046502 (2009).

[52] H. Kim, S. M. Thon, P. M. Petroff, and D. Bouwmeester, Appl. Phys. Lett. **95**, 243107 (2009).

[53] M. Tavis and F. W. Cummings, Phys. Rev. **170**, 379 (1968).

[54] E. Jaynes and F. Cummings, Proc. IEEE **51**, 89 (1963).

[55]Y. Yamamoto and A. Imamoğlu, *Mesoscopic Quantum Optics* (Wiley, New York,1999).
[56]S. Reitzenstein and A. Forchel, J. Phys. D: Appl. Phys. **43**, 033001 (2010).
[57]D. Sanvitto, F. P. Laussy, F. Bello, D. M. Whittaker, A. M. Fox, M. S. Skolnick, A. Tahraoui, P. W. Fry, and M. Hopkinson, e-print arXiv:cond-mat/0612034 (unpublished).
[58]A. Gonzalez-Tudela, E. del Valle, C. Tejedor, and F. Laussy, Superlattices Microstruct. **47**, 16 (2010).
[59]R. J. Thompson, G. Rempe, and H. J. Kimble, Phys. Rev. Lett. **68**, 1132 (1992).
[60]H. Walther, B. T. H. Varcoe, B.-. Englert, and T. Becker, Rep. Prog. Phys. **69**, 1325 (2006).
[61]A. Wallraff, D. I. Schuster, A. Blais, L. Frunzio, R.-S. Huang, J. Majer, S. Kumar, S. M. Girvin, and R. J. Schoelkopf, Nature (London) **431**, 162 (2004).
[62]J. M. Fink, R. Bianchetti, M. Baur, M. Goeppl, L. Steffen, S. Filipp, P. J. Leek, A. Blais, and A. Wallraff, Phys. Rev. Lett. **103**, 083601 (2009).
[63]S. Filipp, M. Göppl, J. M. Fink, M. Baur, R. Bianchetti, L. Steffen, and A. Wallraff, Phys. Rev. A**83**, 063827 (2011).
[64]Y.-S. Park, A. K. Cook, and H. Wang, Nano Lett. **6**, 2075 (2006).
[65]C. Santori, P. E. Barclay, K.-M. C. Fu, R. G. Beausoleil, S. Spillane, and M. Fisch, Nanotechnology **21**, 274008 (2010).
[66]D. Englund, B. Shields, K. Rivoire, F. Hatami, J. Vuckovic, H. Park, and M. D. Lukin, Nano Lett. **10**, 3922 (2010).
[67]D. Press, S. Götzinger, S. Reitzenstein, C. Hofmann, A. Löffler, M. Kamp, A. Forchel, and Y. Yamamoto, Phys. Rev. Lett. **98**, 117402 (2007).
[68]M. Kaniber, A. Laucht, A. Neumann, J. M. Villas-Boas, M. Bichler, M.-C. Amann, and J. J. Finley, Phys. Rev. B **77**, 161303(R) (2008).
[69]M. Winger, T. Volz, G. Tarel, S. Portolan, A. Badolato, K. J. Hennessy, E. L. Hu, A. Beveratos, J. Finley, V. Savona, and A. Imamoğlu, Phys. Rev. Lett. **103**, 207403 (2009).
[70]U. Hohenester, A. Laucht, M. Kaniber, N. Hauke, A. Neumann, A. Mohtashami, M. Seliger, M. Bichler, and J. J. Finley, Phys. Rev. B **80**, 201311(R) (2009).
[71]N. Chauvin, C. Zinoni, M. Francardi, A. Gerardino, L. Balet, B. Alloing, L. H. Li, and A. Fiore, Phys. Rev. B **80**, 241306(R) (2009).
[72]A. Laucht, M. Kaniber, A. Mohtashami, N. Hauke, M. Bichler, and J. J. Finley, Phys. Rev. B **81**, 241302(R) (2010).
[73]A. Gonzalez-Tudela, E. del Valle, E. Cancellieri, C. Tejedor, D. Sanvitto, and F. P. Laussy, Opt. Express **18**, 7002 (2010).
[74]M. O. Scully and M. S. Zubairy, *Quantum Optics* (Cambridge University Press, Cambridge, UK, 1997).
[75]J. H. Eberly and Wódkiewicz, J. Opt. Soc. Am. **67**, 1252 (1977).
[76]H. J. Carmichael, R. J. Brecha, M. G. Raizen, H. J. Kimble, and P. R. Rice, Phys. Rev. A **40**, 5516 (1989).
[77]E. del Valle, *Microcavity Quantum Electrodynamics* (VDM Verlag, Saarbrücken, 2010).
[78]S. Hughes, P. Yao, F. Milde, A. Knorr, D. Dalacu, K. Mnaymneh, V. Sazonova, P. J. Poole, G. C. Aers, J. Lapointe, R. Cheriton, and R. L. Williams, Phys. Rev. B **83**, 165313 (2011).
[79]E. del Valle and F. P. Laussy, Phys. Rev. Lett. **105**, 233601 (2010).
[80]E. del Valle and F. P. Laussy, Phys. Rev. A **84**, 043816 (2011).
[81]E. del Valle, Phys. Rev. A **81**, 053811 (2010).
[82]L. Mandel and E. Wolf, *Optical Coherence and Quantum Optics* (Cambridge University Press, Cambridge, UK, 1995).
[83]R. H. Dicke, Phys. Rev. **93**, 99 (1954).
[84]V. V. Temnov and U. Woggon, Opt. Express **17**, 5774 (2009).